Perturbative analytical treatment of adiabatically moderated soliton self-frequency shift

A. M. Zheltikov*

Physics Department, International Laser Center, M. V. Lomonosov Moscow State University, Vorob'evy gory, Moscow 119992, Russia

(Received 2 May 2006; published 28 March 2007)

We provide a perturbative analytical treatment of the soliton self-frequency-shift (SSFS) in optical fibers including the main physical mechanisms limiting the SSFS, such as the high-order dispersion, the wavelength dependence of the effective mode area, and optical loss. We use this approach to estimate the frequency shift of a soliton with adiabatically varying local parameters and compare this estimate with the results of numerical simulations for SSFS in photonic-crystal fibers. This comparison shows that, in many situations of practical interest, the proposed approach can adequately predict important tendencies of SSFS, and allows a fair estimation of characteristic length scales for the mechanisms limiting the SSFS.

DOI: 10.1103/PhysRevE.75.037603 PACS number(s): 42.65.Wi

Optical solitons propagating in media with noninstantaneous nonlinear response experience reshaping and continuous frequency down-shifting due to the Raman effect [1,2]. This phenomenon, called soliton self-frequency shift (SSFS) [3], provides a convenient way of generating ultrashort pulses with a tunable carrier frequency. Photonic-crystal fibers (PCFs) [4,5] substantially enhance this nonlinear-optical process [6] due to a strong field confinement in a small-size fiber core [7] and the possibility to tailor dispersion of guided modes by varying the fiber structure [8]. The Raman effect in such fibers can give rise to wavelength shifts of 600–700 nm within propagation lengths of 15–20 cm [6,9,10], suggesting the ways toward the creation of efficient practical fiber-optic sources of frequency-tunable ultrashort pulses for spectroscopic, microscopic, and bioimaging applications [11]. Redshifted soliton signals formed by sub-6-fs laser pulses in PCFs have been demonstrated to allow a synchronized seeding of a picosecond Nd:YAG pump laser, permitting a considerable simplification of a few-cycle-pulse optical parametric chirped-pulse amplification (OPCPA) [12].

A high sensitivity of the SSFS to the power of the input pulse may cause serious difficulties in SSFS-based optical schemes, as input power fluctuations are transformed in this regime into unwanted variations in the central wavelength and the timing jitter of the frequency-shifted pulse at the output of the fiber. Under these circumstances, it becomes difficult to precisely match the spectrum of the PCF output with spectral characteristics of the following cascades, such as the gain band of an amplifier, as in the OPCPA scheme [12], or transmission band of filters in spectroscopic measurements [13]. Luckily, there are several physical mechanisms that tend to limit the SSFS after a certain propagation length, helping to reduce wavelength uncertainties and the timing jitter of the frequency-shifted soliton at the output of the fiber. The generalized nonlinear Schrödinger equation (GNSE) [14] has been intensely used since the mid 1980s to analyze the main tendencies in the SSFS [15,16], including the decrease in the soliton frequency shift rate caused by the wavelength dependence of the fiber group-velocity dispersion (GVD), which typically tends to increase toward longer wavelengths for conventional optical fibers, increasing the soliton pulse width. In earlier related work, Mamyshev and Chernikov [17] have included the third-order dispersion and the frequency-dependent effective mode area $A_{\mathrm{eff}}(\lambda)$ in the pulse-evolution equation to find that the $A_{\mathrm{eff}}(\lambda)$ dependence reduces the SSFS relative to fibers with a frequency-independent mode area. Karasawa *et al.* [18] have extended the analysis to few-cycle pulses, showing that the wavelength dependence of the effective mode area can give rise to observable effects in the waveguide spectral broadening of few-cycle laser pulses. Kibler *et al.* [19] have analyzed the GNSE with a wavelength-dependent mode area, demonstrating that the $A_{\mathrm{eff}}(\lambda)$-related effects may become noticeable in spectral transformation and supercontinuum generation processes in PCFs in the regimes where the Raman effect gives rise to large frequency shifts, pushing the soliton into the infrared region. In PCFs, the balance between diffraction and index-step guiding can be controlled by modifying the fiber structure, leading to substantially different wavelength dependences of the effective mode area $A_{\mathrm{eff}}(\lambda)$, thus offering the way to control the SSFS of ultrashort laser pulses down to a few-cycle regime [20].

In this work, we provide an approximate perturbative analytical treatment of the SSFS in optical fibers including the main physical mechanisms limiting the SSFS. Our main goal here is to reexamine the already known physics behind the SSFS using the standard framework of the nonlinear Schrödinger equation and to apply the results of this analysis to the problems of current interest, including the nonlinear-optical transformation of ultrashort pulses in PCFs in first place. We will find a simple estimate for the SSFS assuming that high-order dispersion, the wavelength dependence of the effective mode area, and optical loss give rise to adiabatically slow variations in the local parameters of a soliton. Comparison of this estimate with the results of GNSE-based numerical simulations for SSFS in PCFs shows that, in many situations of practical interest, the proposed approach can adequately reproduce important tendencies of SSFS, thus providing a useful tool for estimating the main parameters of wavelength-shifting solitons and giving useful insights into the tendencies of soliton dynamics in various types of optical fibers.

We start with the basic relations for SSFS derived in the seminal work by Gordon [21]. The method proposed by Gor-

*Electronic address: zheltikov@phys.msu.ru

don involves a spectral transformation of the nonlinear Schrödinger equation (NSE)

$$-i\frac{\partial u}{\partial z}=\frac{1}{2}\frac{\partial^2 u}{\partial t^2}+|u|^2u \tag{1}$$

for the field envelope u. Dimensionless time t_s and length z_s in Eq. (1) are defined as $t_s^2/z_s=\lambda^2 D/2\pi c=-\partial^2\beta/\partial\omega^2$ and $P_s z_s=\lambda A_{\text{eff}}/2\pi n_2$, where λ and ω are the wavelength and frequency, P_s is the soliton power, D is the group-velocity dispersion (GVD), β and A_{eff} are the propagation constant and the effective mode area, n_2 is the nonlinear refractive index of the fiber material, and c is the speed of light in vacuum.

The soliton solution to Eq. (1) is written as $u=\text{sech}(t)\exp(iz/2)$. The pulse width of such a soliton defined at half-maximum of its temporal power profile is $\tau=1.763t_s$. Retarded nonlinear response of the medium is included in the model [21,22] by modifying the nonlinear term on the right-hand side of Eq. (1),

$$-i\frac{\partial u}{\partial z}=\frac{1}{2}\frac{\partial^2 u}{\partial t^2}+u(t)\int f(\eta)|u(t-\eta)|^2 d\eta, \tag{2}$$

where $f(\eta)$ is the real function governing the Raman response of the fiber material. Fourier transform of this function recovers the optical susceptibility of the medium, $\chi(\Omega)=\int f(\eta)\exp(i\Omega\eta)d\eta$. As shown in Refs. [21,22], a Taylor series expansion of $|u(t-\eta)|^2$ around t up to the first order in s reduces Eq. (2) to

$$-i\frac{\partial u}{\partial z}=\frac{1}{2}\frac{\partial^2 u}{\partial t^2}+|u|^2u-\chi u\frac{\partial|u|^2}{\partial t} \tag{3}$$

with $\chi=\int\eta f(\eta)d\eta$. This approximation implies that the decay time of the Raman response is much shorter than the pulse width [22].

Spectral transformation of Eq. (2) yields the following expression for the SSFS rate in THz/km [21]:

$$\frac{d\nu}{dz}\approx-\frac{\mu\lambda^2 D}{t_s^3}\int_0^\infty \Omega^3 R(\Omega/2\pi t_s)/\sinh^2(\pi\Omega/2)d\Omega, \tag{4}$$

where ν is the shift of the central frequency of the soliton, μ is a factor, and $R(\Omega/2\pi t_s)=\alpha_R(\Omega)$.

A linear approximation of the function $R(\xi)$ [$R(\xi)\approx 0.492(\xi/13.2)$ for fused silica] gives the celebrated Gordon formula [21] for the rate of the soliton frequency shift ν [23],

$$\frac{d\nu}{dz}\approx-\frac{\kappa_G}{\tau^4}, \tag{5a}$$

where $\kappa_G=\kappa_G(\lambda,D)=\sigma_0\lambda D$ and σ_0 is a constant. For $\lambda=1.5\ \mu$m and $D=15$ ps/nm/km, Eq. (6a) gives [21] $d\nu/dz(\text{THz/km})\approx 0.0436/\tau^4$, where τ is measured in picoseconds.

Since in laser experiments, the spectral intensity is most often measured as a function of radiation wavelength, it is convenient to introduce the wavelength shift $\delta\lambda=\lambda-\lambda_0$, defined as the deviation of the current (local) central wavelength of the soliton λ from its initial central wavelength λ_0, and transform Eq. (5a) to the form allowing direct calculation of $\delta\lambda$,

$$\frac{d(\delta\lambda)}{dz}\approx\frac{\lambda_0^2}{c}\frac{\kappa_G}{\tau^4}. \tag{5b}$$

The Gordon formula gives the key for identifying important tendencies of SSFS and explaining the basic physics behind this phenomenon. Lucek and Blow [24] have demonstrated that it is possible to generalize the Gordon relation to fibers with a loss by considering τ as a local soliton pulse width, which depends, because of fiber loss, on the propagation coordinate z. Other important factors changing the local soliton pulse width include, as is seen from the definitions of t_s and z_s, high-order dispersion and the wavelength dependence of the effective mode area A_{eff},

$$\tau^2=\tau^2(\lambda,z)\propto\frac{\lambda^3 D A_{\text{eff}}}{P_s(z)}. \tag{6}$$

Along with the explicit wavelength dependence, Eq. (6) involves the GVD and the effective mode area, which change because of high-order dispersion and diffraction, respectively, as the central frequency of the soliton is shifted due to the Raman effect. Guided modes are typically more compact for short wavelengths and are characterized by a larger effective area in the long-wavelength range. The influence of the above-specified factors can become quite dramatic for SSFS in PCFs, where the Raman effect can shift the central wavelength of a soliton by hundreds of nanometers within tens of centimeters of fiber length.

In our qualitative analysis, we include the wavelength dependences of the GVD and the effective mode area by expressing D through $\beta_2=\partial^2\beta/\partial\omega^2$, $D=-(2\pi c/\lambda^2)\beta_2$, and consider small variations in the central wavelength of the soliton λ, the effective mode area A_{eff}, and parameter β_2 caused by the shift of the soliton from the initial central wavelength λ_0,

$$\lambda^2\approx\lambda_0^2[1-(2\lambda_0/c)\nu], \tag{7}$$

$$A_{\text{eff}}^2\approx A_0^2(1-2\xi\nu), \tag{8}$$

$$\beta_2\approx\beta_{20}[1-(2\pi\beta_{30}/|\beta_{20}|)\nu], \tag{9}$$

where $A_0=A_{\text{eff}}(\lambda_0)$, $\beta_{20}=\beta_2(\lambda_0)$, $\xi=-A_0^{-1}(\partial A_{\text{eff}}/\partial\nu)|_{\lambda=\lambda_0}$, and $\beta_{30}=\partial^3\beta/\partial\omega^3|_{\lambda=\lambda_0}$ is the third-order dispersion coefficient.

To include the fiber loss, we assume that the soliton power $P_s(z)$ in Eq. (6) decreases exponentially along the fiber, $P_s(z)=P_0\exp(-\alpha z)$, where α is the fiber loss and P_0 is the initial soliton power. Substituting the power series (7)–(9) into Eq. (6), we then arrive at

$$\frac{d\nu}{dz}\approx-\frac{\kappa_0}{\tau_0^4}(1+\theta\nu)\exp(-2\alpha z) \tag{10a}$$

or

$$\frac{d(\delta\lambda)}{dz}\approx\frac{\kappa_0}{\tau_0^4}\frac{\lambda_0^2}{c}(1+\theta\nu)\exp(-2\alpha z), \tag{10b}$$

where $\theta=2(\lambda_0/c+\xi+\psi)$, $\psi=\pi\beta_{30}/|\beta_{20}|$, $\kappa_0=\kappa_G(\lambda_0,D_0)$, and $\tau_0=\tau(\lambda_0,0)$.

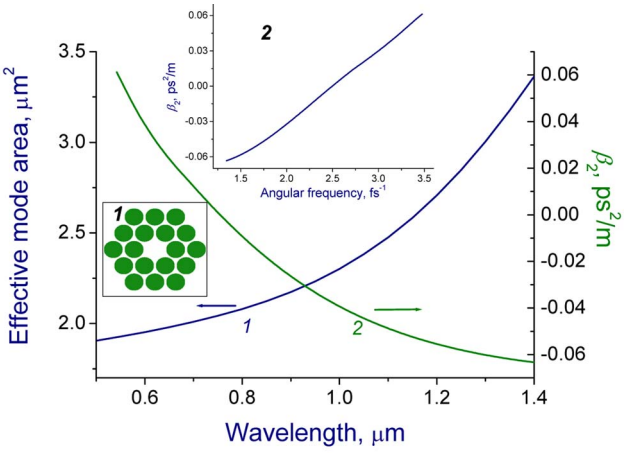

FIG. 1. (Color online) Wavelength dependences of the effective mode area (line 1) and group-velocity dispersion parameter β_2 (line 2) for a fused silica photonic-crystal fiber with a cross-section structure shown in inset 1. Inset 2 displays the parameter β_2 as a function of the angular frequency ω.

Integration of Eqs. (10a) and (10b) yields the following expressions for the soliton frequency and wavelength shifts:

$$\nu(z) = \frac{1}{\theta}\left[\exp\left(-\theta\frac{\kappa_0}{\tau_0^4}z_{\text{eff}}\right) - 1\right] \tag{11a}$$

$$\delta\lambda(z) = -\frac{1}{\theta}\frac{\lambda_0^2}{c}\left[\exp\left(-\theta\frac{\kappa_0}{\tau_0^4}z_{\text{eff}}\right) - 1\right], \tag{11b}$$

where

$$z_{\text{eff}} = \frac{1}{2\alpha}[1 - \exp(-2\alpha z)]. \tag{12}$$

In the regime where αz, $\theta\kappa_0\tau_0^{-4}z \ll 1$, Eq. (11a) is reduced to the Gordon formula (5a). However, as the soliton propagates further on along the fiber, its central wavelength is shifted, leading to changes in the GVD and the effective mode area. For fiber lengths approaching half the attenuation length, fiber loss also come into play, leading to a further suppression of SSFS. To quantify the impact of each of these factors on SSFS, we introduce the following spatial scales: $l_\lambda = c\tau_0^4(2\lambda_0\kappa_0)^{-1}$, $l_\xi = \tau_0^4(2\xi\kappa_0)^{-1}$, $l_D = \tau_0^4|\beta_{20}|(2\pi\beta_{30}\kappa_0)^{-1}$, and $l_\alpha = (2\alpha)^{-1}$. The length scale l_λ is related to the variation of the central wavelength of the soliton. The length l_D characterizes a changing dispersion sensed by the soliton. The length l_ξ is responsible for the diffraction mechanism of SSFS limitation, as it is controlled by the variation in the effective mode area A_{eff}, reflecting the changing balance between diffraction and index-step field confinement in a waveguide mode. Finally, the length l_α is fully determined by the fiber loss and is insensitive to soliton parameters.

We now apply the results of our perturbative treatment to understand the main tendencies in the evolution of redshifting solitons in a generic-type PCF (inset 1 in Fig. 1) with wavelength dependences of the effective mode area and the GVD shown by curves 1 and 2 in Fig. 1. In order to expand the applicability range of Eq. (9), we choose a fiber structure that provides a dispersion profile with a weakly varying β_3 within the range of wavelengths from 0.54 to 1.26 μm (see inset 2 in Fig. 1).

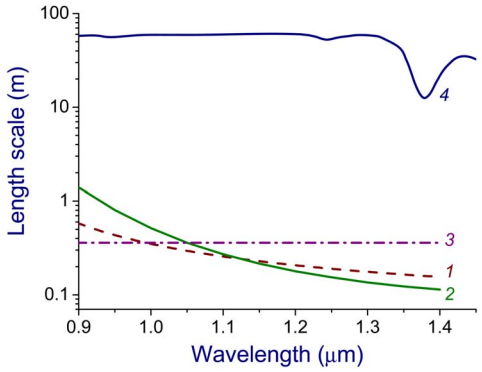

FIG. 2. (Color online) Characteristic lengths l_λ (curve 1), l_ξ (curve 2), l_D (curve 3), and l_α (curve 4) calculated as functions of the wavelength λ_0 for a fused silica PCF with the wavelength dependences of the effective mode area and GVD shown in Fig. 1.

Curves 1, 2, and 3 in Fig. 2 display the characteristic lengths l_λ, l_ξ, and l_D calculated as functions of the wavelength λ_0 for the PCF with the wavelength dependences of A_{eff} and GVD shown in Fig. 1. It can be seen from the comparison of these curves that, at the initial stage of SSFS, high-order dispersion is the main factor that limits the SSFS. However, as the soliton is shifted toward longer wavelengths, the diffraction mechanism plays a progressively important role, becoming a dominant factor of SSFS suppression in the near-IR range (for $\lambda_0 > 1.3$ μm in Fig. 2). Curve 4 in Fig. 2 shows a typical wavelength dependence of the characteristic length scale l_α for a silica PCF [4,25]. Comparison of this plot with curves 1–3 in the same figure shows that the fiber loss is typically much less significant for the suppression of SSFS in silica PCFs. This relation between the characteristic length scales may, however, change for PCFs made of highly nonlinear glasses, where material losses are usually much higher.

In Fig. 3, we compare the soliton wavelength shift calculated with the use of Eqs. (10)–(11) and (12) with the results

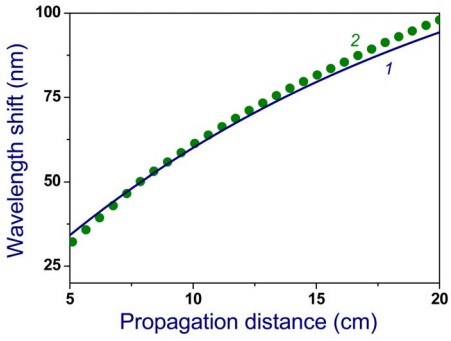

FIG. 3. (Color online) The soliton wavelength shift calculated with the use of Eqs. (12)–(14) (curve 1) and by means of numerical solution of the generalized nonlinear Schrödinger equation (curve 2) for laser pulses with an initial pulse width of 30 fs, input pulse energy of 0.1 nJ, and the initial central wavelength of 800 nm propagating in a silica PCF with the wavelength dependences of the effective mode area and GVD shown in Fig. 1.

of numerical solution of the GNSE with the PCF dispersion profile included through a sixth-order polynomial fit and retarded nonlinearity described in terms of the standard, dumped-oscillator model of the Raman response [14,22] with an oscillation period of 78.5 fs and a decay time of 32 fs. Calculations were performed for laser pulses with an initial pulse width of 30 fs, input pulse energy of 0.1 nJ, and the initial central wavelength of 800 nm propagating in a silica PCF with the effective mode area and GVD profiles shown in Fig. 1. For the first few centimeters of the fiber, numerical simulations reveal complicated spectral and temporal transformations of the laser pulse dominated by four-wave mixing (FWM) [10], resulting in the generation of an intense Stokes sideband around 900 nm. This part of the field becomes a soliton with an initial pulse width of about 25 fs. The z-coordinate is measured from the point where this soliton is clearly visible in the time domain with the corresponding peak observed in the spectrum at 900 nm. The Raman-effect-induced wavelength shift of this soliton measured with respect to 900 nm is shown as a function of the propagation length by filled circles in Fig. 3.

The solid line (curve 1) in Fig. 3 presents the results of calculations performed with the use of Eqs. (10)–(11) and (12) for the effective mode area and GVD profiles shown in Fig. 1. The initial central wavelength in these calculations is set equal to $\lambda_0=900$ nm, corresponding to $\beta_{20} \approx -0.026$ ps^2/m, $\beta_{30} \approx 3.8\times10^{-5}$ ps^3/m, and $A_0 \approx 2.2$ μm^2. For the chosen set of parameters, our analytical approach, as can be seen from Fig. 3, provides quite adequate predictions for the soliton wavelength shift. A satisfactory agreement between numerical simulations (curve 2) and predictions of our analytical approach (curve 1) holds, however, only within a limited range of propagation lengths. For large z, corresponding to large soliton frequency shifts, Taylor-series expansions of Eqs. (7)–(9) can no longer provide adequate approximations for the local soliton parameters, and a new set of input parameters must be defined for the analytical approach to provide reasonable predictions for the soliton frequency shift.

We have thus applied an approximate perturbative analytical treatment of soliton self-frequency shift in optical fibers to find a simple estimate for the SSFS assuming that high-order dispersion, the wavelength dependence of the effective mode area, and optical loss give rise to adiabatically slow variations in the local parameters of a soliton. Comparison of this estimate with the results of numerical simulations for SSFS in PCFs shows that, in many situations of practical interest, the proposed approach can adequately reproduce important tendencies of SSFS, allowing, in particular, an assessment of characteristic lengths for the main physical mechanisms limiting the SSFS in an optical fiber.

Illuminating discussions with E.E. Serebryannikov are gratefully acknowledged. This study was supported in part by the Russian Foundation for Basic Research (Contracts Nos. 06-02-16880 and 05-02-90566-NNS) and INTAS (Contracts Nos. 03-51-5037 and 03-51-5288). The research described in this paper was made possible in part by Grant No. RUP2-2695 of the U.S. Civilian Research and Development Foundation for the Independent States of the Former Soviet Union (CRDF).

[1] F. M. Mitschke and L. F. Mollenauer, Opt. Lett. **11**, 659 (1986).
[2] E. M. Dianov, A. Y. Karasik, P. V. Mamyshev, A. M. Prokhorov, V. N. Serkin, M. F. Stel'makh, and A. A. Fomichev, JETP Lett. **41**, 294 (1985).
[3] G. P. Agrawal, *Nonlinear Fiber Optics* (Academic, San Diego, 2001).
[4] P. St. J. Russell, Science **299**, 358 (2003).
[5] J. C. Knight, Nature (London) **424**, 847 (2003).
[6] X. Liu, C. Xu, W. H. Knox, J. K. Chandalia, B. J. Eggleton, S. G. Kosinski, and R. S. Windeler, Opt. Lett. **26**, 358 (2001).
[7] A. B. Fedotov, A. M. Zheltikov, A. P. Tarasevitch, and D. von der Linde, Appl. Phys. B: Lasers Opt. **73**, 181 (2001).
[8] W. H. Reeves, D. V. Skryabin, F. Biancalana, J. C. Knight, P. St. J. Russell, F. G. Omenetto, A. Efimov, and A. J. Taylor, Nature (London) **424**, 511 (2003).
[9] E. E. Serebryannikov, A. M. Zheltikov, N. Ishii, C. Y. Teisset, S. Köhler, T. Fuji, T. Metzger, F. Krausz, and A. Baltuška, Appl. Phys. B: Lasers Opt. **81**, 585 (2005).
[10] E. E. Serebryannikov, A. M. Zheltikov, N. Ishii, C. Y. Teisset, S. Köhler, T. Fuji, T. Metzger, F. Krausz, and A. Baltuška, Phys. Rev. E **72**, 056603 (2005).
[11] D. A. Sidorov-Biryukov, E. E. Serebryannikov, and A. M. Zheltikov, Opt. Lett. **31**, 2323 (2006).
[12] C. Y. Teisset, N. Ishii, T. Fuji, T. Metzger, S. Köhler, R. Holzwarth, A. Baltuska, A. M. Zheltikov, and F. Krausz, Opt. Express **13**, 6550 (2005).
[13] S. O. Konorov, D. A. Akimov, E. E. Serebryannikov, A. A. Ivanov, M. V. Alfimov, and A. M. Zheltikov, Phys. Rev. E **70**, 057601 (2004).
[14] K. J. Blow and D. Wood, IEEE J. Quantum Electron. **25**, 2665 (1989).
[15] W. Hodel and H. P. Weber, Opt. Lett. **12**, 924 (1987).
[16] P. Beaud, W. Hodel, B. Zysset, and H. P. Weber, IEEE J. Quantum Electron. **23**, 1938 (1987).
[17] P. V. Mamyshev and S. V. Chernikov, Opt. Lett. **15**, 1076 (1990).
[18] N. Karasawa, S. Nakamura, N. Nakagawa, M. Shibata, R. Morita, H. Shigekawa, and M. Yamashita, IEEE J. Quantum Electron. **37**, 398 (2001).
[19] B. Kibler, J. M. Dudley, and S. Coen, Appl. Phys. B: Lasers Opt. **81**, 337 (2005).
[20] E. E. Serebryannikov, A. M. Zheltikov, S. Köhler, N. Ishii, C. Y. Teisset, T. Fuji, F. Krausz, and A. Baltuška, Phys. Rev. E **73**, 066617 (2006).
[21] J. P. Gordon, Opt. Lett. **11**, 662 (1986).
[22] R. H. Stolen, J. P. Gordon, W. H. Tomlinson, and H. A. Haus, J. Opt. Soc. Am. B **6**, 1159 (1989).
[23] As highlighted in Ref. [21], a linear approximation of $R(\xi)$ is equivalent to adding the term $-\chi u \partial|u|^2/\partial t$ on the right-hand side of Eq. (1). However, Eq. (5) is more general, as it was derived from a more general propagation equation (4).
[24] J. K. Lucek and K. J. Blow, Phys. Rev. A **45**, 6666 (1992).
[25] http://www.crystal-fibre.com/